

Intrinsic Randomness and Spontaneous Symmetry-Breaking in Explosive Systems

G. Nicolis¹ and F. Baras¹

Received May 15, 1987

The effect of fluctuations of either thermodynamic or environmental origin on ignition in explosive systems is analyzed, with special emphasis on thermal explosion. A simple model due to Semenov is first analyzed in the zero-dimensional approximation. It is shown that the ignition times exhibit a wide dispersion, which at the level of the probability distribution of temperature shows up as a transient bimodality. Next, an extension to a spatially distributed system is developed. It is shown that fluctuations induce unexpected symmetry-breaking phenomena, reflected by a considerable dispersion of the position of the first "hot spot" initiated in the system.

KEY WORDS: Fluctuations; combustion; explosive systems; transient bimodality.

1. INTRODUCTION

At some stage of their time development, physicochemical systems may undergo a sudden *switching* between two distinctly different levels of a state variable, preceded by a slow *induction* period and followed by a slow *saturation* characteristic of the final approach toward the stable attractor (Fig. 1). Explosive behavior in connection with thermal or chemical combustion,⁽¹⁾ the growth of a nucleus in a metastable medium,⁽²⁾ switching in nonlinear optical or electronic devices,^(3,4) and logistic growth in population dynamics⁽⁵⁾ provide some characteristic examples of this highly nonlinear behavior.

In some respects the mechanisms giving rise to sudden switching are simpler than those responsible for, say, chemical oscillations, waves, or chaos.^(6,7) For one thing, the system need not possess more than one attractor, nor undergo complex bifurcation cascades. As a matter of fact, it

¹ Faculté des Sciences, Université Libre de Bruxelles, 1050 Bruxelles, Belgium.

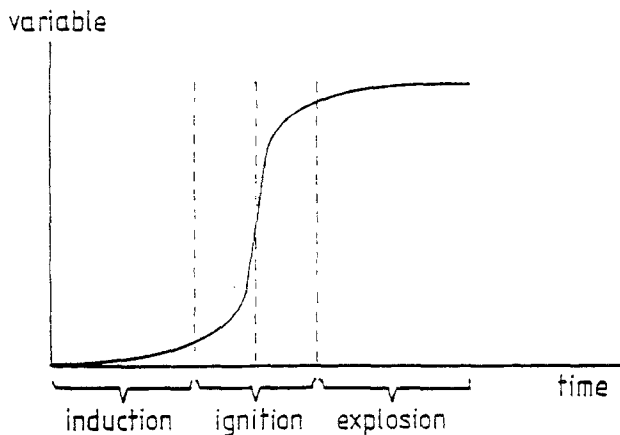


Fig. 1. Typical time dependence associated with explosive behavior.

need not even be an open system maintained permanently out of equilibrium by suitable constraints. For instance, thermal explosion in a closed vessel⁽⁸⁾ in the limit of a high activation energy is an excellent example of the behavior depicted in Fig. 1. As regards systems under permanent nonequilibrium constraint, a typical situation giving rise to switching is depicted in Fig. 2. Here the system is started in a range of initial conditions and parameter values ($\lambda = \lambda_0$) close to a limit-point bifurcation ($\lambda = \lambda_c$). Due to the presence of a zero eigenvalue of the linearized stability problem at λ_c , the first stages of the evolution are slow. As, however, the only attractor available [upper branch in Fig. 2] is at large distance from the initial condition, a sudden jump is bound to occur sooner or later, removing the system from the vicinity of the limit point.^(9,10)

Our principal objective in this article is to show that during the switching process the system is characterized by a high sensitivity to perturbations of either internal (thermodynamic fluctuations) or environmental origin. Although the main ideas and results have a rather wide applicability, we shall carry out the detailed analysis in the case of thermal explosion. We shall see that, as a result of the enhanced sensitivity, ignition becomes an intrinsically random event. Furthermore, when spatial degrees of freedom are incorporated in the description, one witnesses unexpected symmetry-breaking phenomena induced entirely by the fluctuations. These lead to marked differentiation in the position and occurrence time of "hot spots", the precursors of the nuclei of combustion. Our results highlight the wide applicability of the concepts of self-organization and order through fluctuations pioneered by Ilya Prigogine.

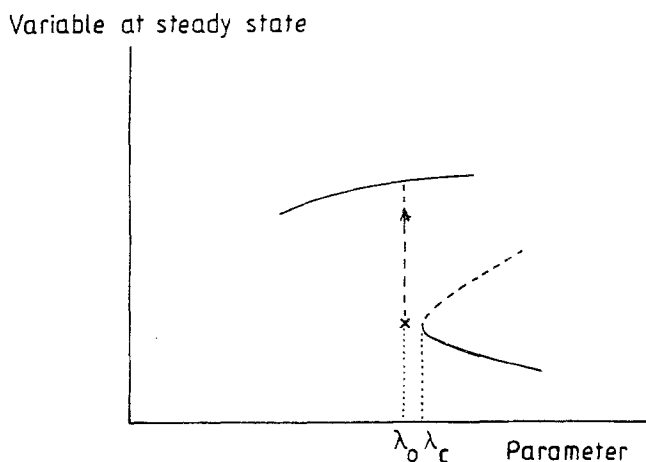


Fig. 2. Parameter range associated with explosive behavior in a state diagram in which the steady state is plotted against a control parameter.

The paper is organized as follows. In Section 2 we set up the stochastic description of the fluctuations in a simple model of thermal combustion due to Semenov. In Section 3 we analyze the behavior in the zero-dimensional limit, in which spatial degrees of freedom are discarded. We find two striking manifestations of the high sensitivity of the system in the ignition region: a broad distribution of ignition times, and a *transient bimodality* of the probability distribution. In Section 4 the problem of combustion in a spatially distributed system subjected to stochastic perturbations is formulated. In Section 5, it is shown that fluctuations induce a wide spatial dispersion of combustion. This stems from the fact that individual realizations of the underlying stochastic process develop spatially inhomogeneous profiles despite the homogeneity of the initial state and the strong invariance properties of the evolution laws. The main conclusions, along with some suggestions, are summarized in Section 6.

2. STOCHASTIC FORMULATION OF THE SEMENOV MODEL: ZERO-DIMENSIONAL APPROXIMATION

We consider a finite reaction vessel of volume V and surface area S , which allows for thermal contact of the reactants with a reservoir at temperature T_0 at the boundary of the vessel, but does not allow for mass flow of the reactants across the boundaries. An exothermic reaction is supposed to occur in the vessel. We assume that the reactants are distributed homogeneously, for instance, by an efficient stirring mechanism, postponing until Sections 4 and 5 the effect of spatial degrees of freedom.

We denote by \bar{c} the concentration of the reactant and by \bar{T} the internal temperature. In the limit in which the thermal relaxation time is much faster than the chemical one, one may neglect the reactant consumption and identify \bar{c} with its initial value c_0 . Assuming a single irreversible m th-order reaction, one obtains, then, the following equation of evolution for \bar{T} :

$$\rho C_V d\bar{T}/dt = Qc_0^m k_0 \exp(-U/R\bar{T}) - \gamma(\bar{T} - T_0) \quad (1)$$

Here ρ and C_V are, respectively, the mass density and specific heat of the system; Q is the heat of reaction; U is the activation energy; R is the gas constant; and $\gamma = \alpha S/V$, α being the Newton cooling coefficient.

It is well known⁽¹⁾ that there exists a range of parameter values for which Eq. (1) admits two simultaneously stable states separated by an intermediate unstable state. However, in the limit of high activation energy, which is the usual situation in combustion,

$$\varepsilon' = RT_0/U \ll 1 \quad (2)$$

the high-temperature "combustion" branch corresponds to unrealistically large values of temperature. On the other hand, the low-temperature "extinction" branch as well as the intermediate unstable branch are well

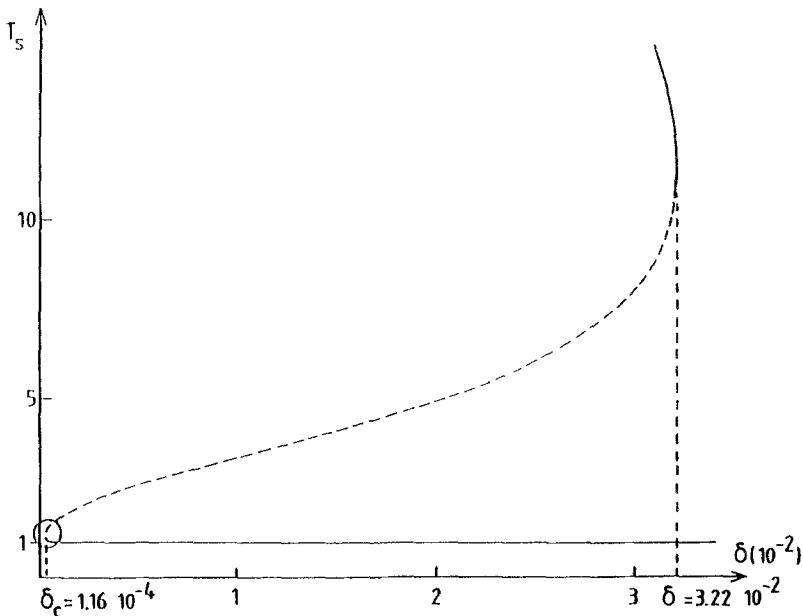


Fig. 3. Multiple steady states in the Semenov model [Eq. (1)]. Parameter value: $\varepsilon' = 0.08$.

described. Figure 3 gives a plot of these latter steady states T_s as a function of the scaled parameter

$$\delta = \gamma/Qc_0^m k_0 \tag{3}$$

Let the system be started in the region of parameter values to the left of the turning point of the lower branch of Fig. 3. One will observe than a thermal explosion, whereby, after an induction period, temperature increases suddenly and tends to the combustion branch of the steady-state diagram, in a way similar to Fig. 1. Because of the unrealistically high value of the latter, we discard the part of the evolution referring to the final saturation, since for that stage the assumption of no consumption of the reactant breaks down. Figure 4 describes the induction period and the first stages of explosion, for which the theory provides a satisfactory description. As δ comes closer to δ_c , ignition becomes sharper in the sense that the initial plateau becomes increasingly longer, or, in other words, ignition time tends to infinity. A straightforward computation yields⁽¹⁰⁾

$$t_i \approx (1 - \delta/\delta_c)^{-1/2} \tag{4}$$

which is analogous to the phenomenon of “critical slowing down” familiar from phase transitions.

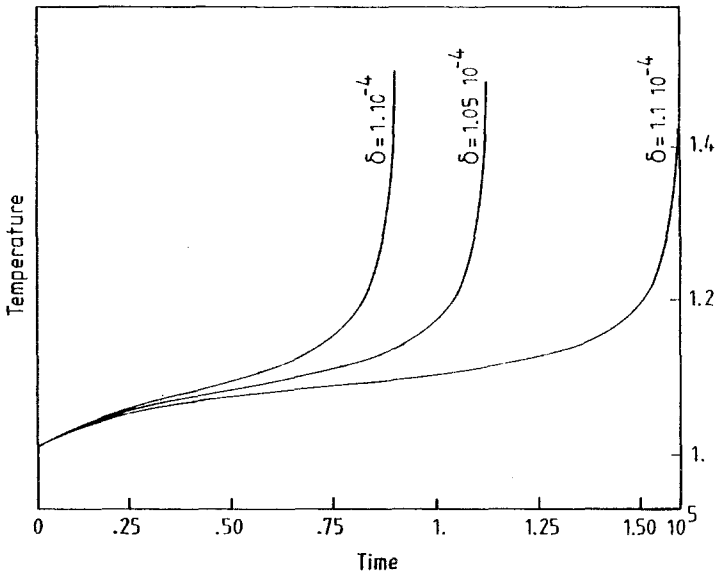


Fig. 4. Thermal explosion behavior to the left of the turning point of Fig. 3. Parameter value as in Fig. 3.

We now turn to the stochastic aspects of the problem.^(11,12) Two kinds of dynamical processes take place simultaneously in the system: a chemical reaction within the vessel and a transport of energy between the vessel and the external reservoir. The master equation for the probability distribution of the energy E can therefore be divided into two parts,

$$\frac{d}{dt} P(E, t) = L_{\text{ch}} + L_{\text{tr}} \quad (5)$$

As usual, we shall model the effect of chemical reactions by a birth and death process.⁽⁶⁾ In the present case of a single irreversible reaction, one deals in fact with a pure birth process for the energy variable, and

$$L_{\text{ch}} = \lambda(E - Q) P(E - Q) - \lambda(E) P(E) \quad (6a)$$

with [cf. Eq. (1)]

$$\lambda(E) = V k_0 c_0^m \exp\left(-\frac{U}{k_B E / N C_V}\right) \quad (6b)$$

where N is the total number of particles. We recall that in the Semenov approximation the reactant consumption is neglected: N must be treated therefore as a constant parameter.

Since the system under consideration possesses a unique attractor, one may capture the main features by reducing L_{ch} to a Fokker-Planck operator,⁽¹³⁾ provided that one expands the stochastic variables around the value given by the deterministic laws of evolution. It is well known that this in turn is equivalent to augmenting the rate law, Eq. (1), by including a chemical random force $F_{\text{ch}}(t)$. A standard calculation⁽¹¹⁻¹³⁾ leads to the following properties:

$$\begin{aligned} \langle F_{\text{ch}}(t) \rangle &= 0 \\ \langle F_{\text{ch}}(t) F_{\text{ch}}(t') \rangle &= \varepsilon Q_{\text{ch}} \delta(t - t') \\ Q_{\text{ch}} &= (Q / \rho C_V)^2 k_0 c_0^m \exp(-U / RT) \end{aligned} \quad (7)$$

where $\varepsilon = V^{-1}$ is the inverse of the size.

We next turn to the stochastic description of the transport process. The evolution operator L_{tr} , Eq. (5), has the form^(12,14)

$$\begin{aligned} L_{\text{tr}} = \int d\varepsilon \{ &W(E_0 + \varepsilon, E - \varepsilon | E_0, E) P(E_0 + \varepsilon, E - \varepsilon) \\ &+ W(E_0 - \varepsilon, E + \varepsilon | E_0, E) P(E_0 - \varepsilon, E + \varepsilon) \\ &- [W(E_0, E | E_0 - \varepsilon, E + \varepsilon) + W(E_0, E | E_0 + \varepsilon, E - \varepsilon)] P(E_0, E) \} \quad (8) \end{aligned}$$

where E_0 denotes the energy of the reservoir and W the transition probability per unit time between two different energy states of the system and the reservoir. As for L_{ch} , we reduce L_{tr} to a Fokker–Planck operator and fix the form of the W 's by requiring that detailed balance be satisfied at equilibrium. This leads to the following properties of the random force $F_{tr}(t)$ associated with the transport:

$$\begin{aligned} \langle F_{tr}(t) \rangle &= 0 \\ \langle F_{tr}(t) F_{tr}(t') \rangle &= \varepsilon Q_{tr} \delta(t - t') \\ Q_{tr} &= [\gamma/(\rho C_V)^2] k_B(\bar{T}^2 + T_0^2) \end{aligned} \tag{9}$$

Summarizing, then, we obtain an augmented Semenov equation incorporating the effect of fluctuations in the form

$$\frac{d}{dt} T = \frac{Q c_0^m k_0}{\rho C_V} \exp\left(\frac{-U}{RT}\right) - \frac{\gamma}{\rho C_V} (T - T_0) + F(t) \tag{10}$$

where $F(t) = F_{ch} + F_{tr}$ is a Gaussian white noise whose strength is allowed to depend on the deterministic solution:

$$\langle F(t) \rangle = 0, \quad \langle F(t) F(t') \rangle = \varepsilon Q_T \delta(t - t') \tag{11}$$

ε being the inverse of the system size. The precise form of Q_T can be determined by adding Q_{ch} and Q_{tr} , Eqs. (7) and (9):

$$Q_T = \frac{Q^2 k_0 c_0^m}{(\rho C_V)^2} \exp\left(\frac{-U}{RT}\right) + \frac{\gamma}{(\rho C_V)^2} k_B(\bar{T}^2 + T_0^2) \tag{12}$$

All desired properties of the fluctuations can be computed from the above equations or from the Fokker–Planck equation for the underlying probability distribution:

$$\frac{\partial}{\partial t} P(T; t) = -\frac{\partial}{\partial T} \left[\frac{\partial \mathcal{U}}{\partial T} P(T; t) \right] + \frac{\varepsilon}{2} Q_T \frac{\partial^2}{\partial T^2} P(T; t) \tag{13}$$

The drift term of this latter equation features the deterministic potential,

$$\mathcal{U} = \int^T dT' \left[\frac{Q c_0^m k_0}{\rho C_V} \exp\left(\frac{-U}{RT'}\right) - \frac{\gamma}{\rho C_V} (T' - T_0) \right] \tag{14}$$

3. IGNITION TIME STATISTICS AND TRANSIENT BIMODALITY

Consider now the spontaneous explosion region, that is, values of δ less than the ignition limit δ_c (see Fig. 3). Figure 5 reports the results of

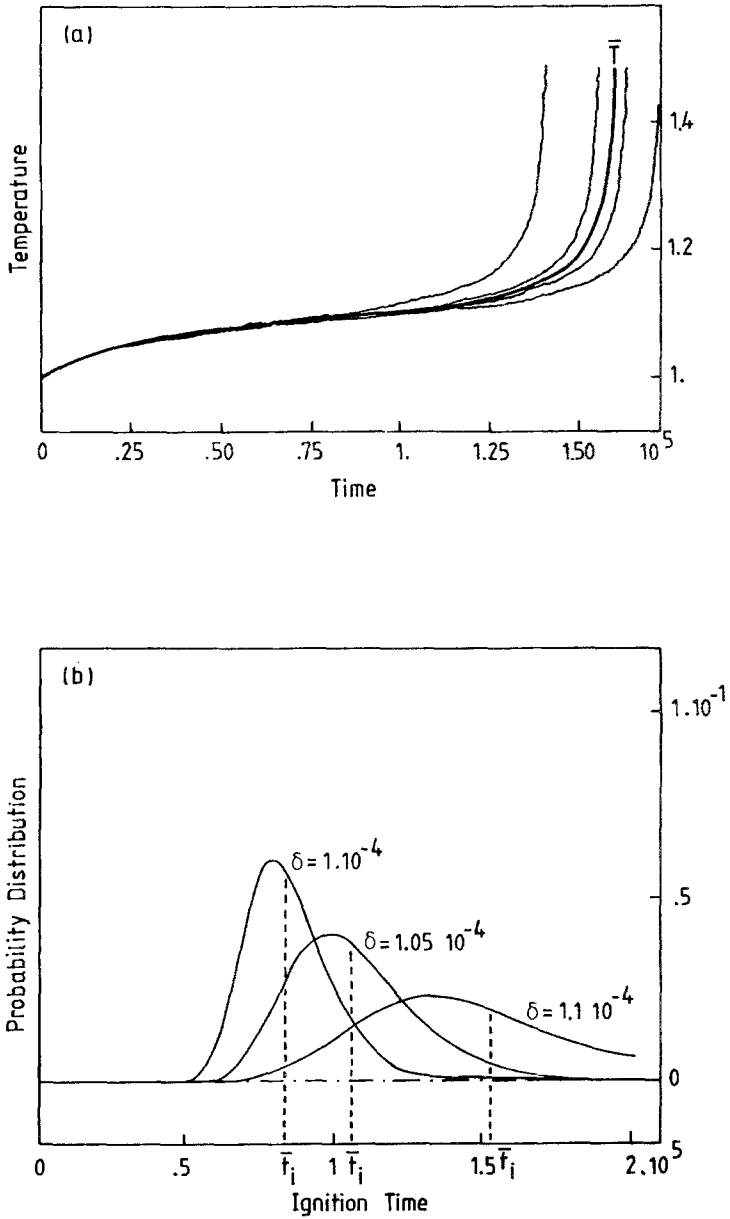


Fig. 5. Two different views of the dispersion of ignition times induced by the fluctuations. (a) Different realizations of the stochastic process, Eq. (10). (b) Probability distribution of ignition times. Parameter values: $\epsilon' = 0.08$, $\epsilon = 0.001$.

numerical solution of the Langevin equation for different δ 's and initial conditions. In each case, the stochastic trajectory is followed and the times at which it crosses a preassigned level of temperature value T_c representative of explosion are determined. This allows one to compute the *probability distribution of ignition times*. We see that far from the ignition point this distribution is narrow, and its peak coincides with the deterministic explosion time. However, as δ approaches the critical (limit point) value δ_c the distribution becomes very broad, and the position of its maximum is substantially different from the deterministic time, which belongs to the tail of the ignition time distribution. In other words, *ignition becomes essentially a random event*. Moreover, fluctuations tend to *advance* the most probable value of ignition time.

Let us outline a qualitative explanation of these results. To this end we compute the mean τ_1 and the variance $\delta\tau_2$ of the first passage time for reaching the critical value T_c , starting from an initial state $T(0)$ close to the reservoir temperature T_0 . Treating T_c and $T=0$, respectively, as an absorbing and as a reflecting barrier, we obtain⁽¹⁵⁾

$$\tau_1(T(0)) = \frac{2}{\varepsilon Q_T} \int_{T(0)}^{T_c} dy \exp \left[\frac{2}{\varepsilon Q_T} \mathcal{U}(y) \right] \int_0^y dz \exp \left[- \frac{2}{\varepsilon Q_T} \mathcal{U}(z) \right] \quad (15)$$

$$\delta\tau_2 = (\tau_2 - \tau_1^2)^{1/2} \quad (16a)$$

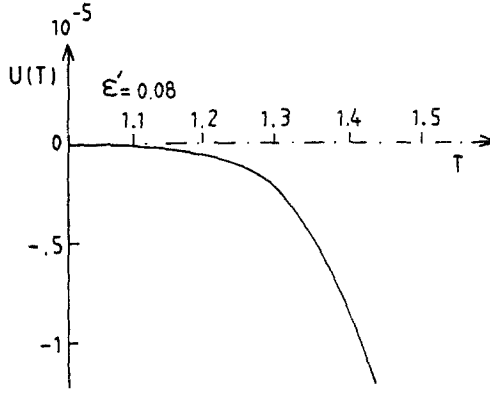
with

$$\frac{\partial}{\partial x} \tau_2(x) + \frac{\varepsilon Q_T}{2} \frac{\partial^2}{\partial x^2} \tau_2(x) = -2\tau_1(x) \quad (16b)$$

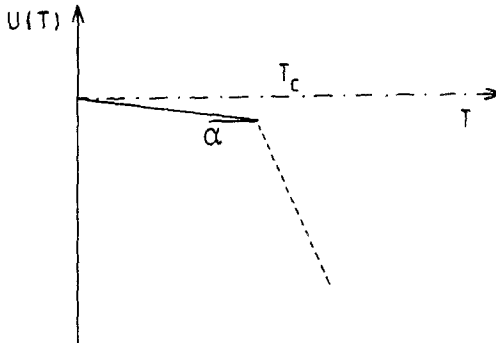
Equations (15) and (16) are in general intractable, in view of the full expression of the kinetic potential [cf. Eq. (14)]. We shall therefore resort to an approximation that allows us to obtain some qualitative information capturing the essence of the phenomenon of interest. Specifically, noting once again that after a first transient the rate of change of the temperature levels off at a very small value during a time period essentially equal to the time of ignition, we approximate the rate law in this range by a fixed, positive parameter α . Clearly, α is a decreasing function of the cooling rate γ and an increasing function of the parameter ε' [cf. Eq. (2)], the ratio of thermal to activation energy. The kinetic potential \mathcal{U} becomes [assuming $\mathcal{U}(0)=0$]

$$\mathcal{U}(T) = -\alpha T; \quad T(0) \leq T < T_c \quad (17)$$

In Fig. 6 the full potential [Eq. (14)] and its approximation provided by Eq. (17) are plotted. We see that the approximate representation is



(a)



(b)

Fig. 6. Kinetic potential [Eq. (14)] and its simplified representation [Eq. (17)] in the Semenov model. Parameter values: $\epsilon' = 0.08$, $\delta = 1.1 \times 10^{-4}$.

reasonable for values of T between T_0 and a value that is as close to T_c as desired, provided that ϵ' is sufficiently small and the system operates close to the limit point of Fig. 3.

Expressions (15) and (16b) may now be evaluated explicitly. The result is

$$\tau_1 = \frac{1}{\alpha} [T_c - T(0)] - \frac{\epsilon Q_T}{2\alpha^2} \left[\exp\left(-\frac{2\alpha T(0)}{\epsilon Q_T}\right) - \exp\left(-\frac{2\alpha T_c}{\epsilon Q_T}\right) \right] \quad (18)$$

$$\delta\tau_2^2 = \frac{\epsilon Q_T}{\alpha^3} [T_c - T(0)] + \mathcal{O}(\epsilon^{-\alpha/\epsilon}); \quad \frac{\epsilon}{\alpha} \ll 1 \quad (19)$$

From Eq. (18) we see that τ_1 is shorter than the deterministic value $[T_c - T(0)]/\alpha$. Moreover, as α decreases with increasing γ , it is predicted that both the advancement of the explosion and the broadening of the probability distribution of ignition times (measured by $\delta\tau_2$) will become increasingly marked with increasing γ . These predictions are in full agreement with the numerical results shown in Fig. 5.

We may push the estimate of the broadening of the distribution somewhat further by evaluating the ratio $\delta\tau_2/\tau_1$. We have

$$(\delta\tau_2)/\tau_1 \approx (\varepsilon Q_T)^{1/2}/\alpha \tag{20}$$

independent of $[T_c - T(0)]$. Now, for the parameter values used in the simulations, $\varepsilon Q_T/\alpha^2$ turns out to be as large as about 0.1, although ε is only 10^{-3} . This gives a dispersion $\delta\tau_2$ that is in qualitative agreement with the numerical results. We see the important role played in the problem by the existence of a slow time scale, which enhances the response of the system to even very weak stochastic perturbations.

Further insight into the intrinsic randomness of the system can be obtained by studying the probability distribution $P(T, t)$ as a function of time. As shown in Fig. 7, starting with a distribution centered on a

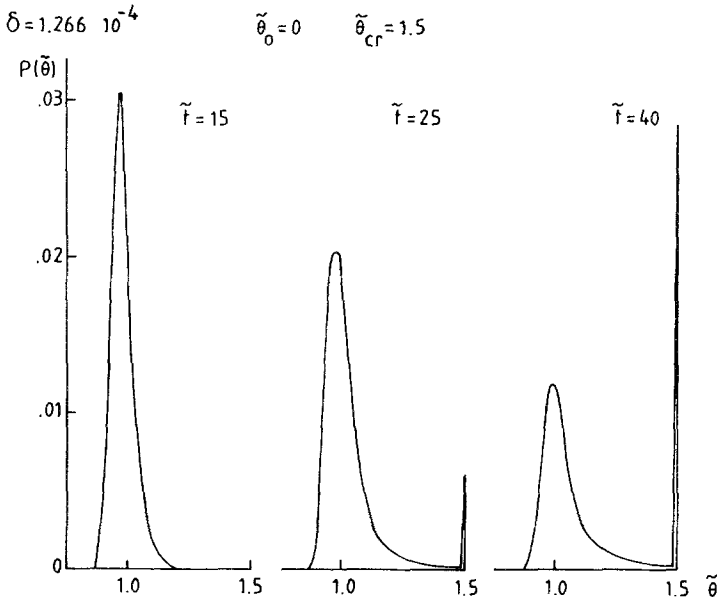


Fig. 7. Successive stages of evolution of the probability distribution $P(\tilde{\theta}, t)$ obtained by numerical solution of the Fokker-Planck equation [cf. Eq. (13)] in which the exponential factor $\exp(-1/\varepsilon'T)$ is approximated by $\exp(\tilde{\theta})$ with $T = 1 + \varepsilon'\tilde{\theta}$ $\{\tilde{t} = (1/\varepsilon')[\exp(-1/\varepsilon')] t\}$. Parameter values: $\delta = 1.266 \times 10^{-4}$, $\varepsilon' = 0.08$, $\varepsilon = 0.001$.

low-temperature state, the system gradually develops a long tail and subsequently a *transient bimodality*, before collapsing again to a unimodal distribution centered on the stable attractor.

Figure 8 outlines a qualitative explanation of this new mechanism of internal variability. Remember that we are dealing with a process involving two time scales, and that our system is initially prepared in a state in which the deterministic rate is very small. The maximum of the underlying probability distribution, whose motion roughly follows the deterministic one, will therefore move very slowly toward the region of higher values of T . Meanwhile, because of the fluctuations, the probability will develop a width proportional to the length of the induction period and inversely proportional to the square root of the size V . If the length of the induction period is large, the size effect will be counteracted and the width will be appreciable. As a result, a substantial part of the probability mass will reach the ignition point well before the maximum does so. At this moment it will be quickly entrained by fast motion toward the region of high values of T , a phenomenon that will be interpreted by the observer as a precocious ignition. This leak of probability will go on continuously, but since the system cannot reach infinite values of temperature, a "traffic jam" will arise, as a result of which a new probability peak will emerge in the region of high T . Eventually the primary peak, by then considerably diminished, will reach the ignition point and this will mark the end of transient bimodality. The same argument suggests that the deterministic ignition time should belong to the tail of the ignition probability distribution, in agreement with the numerical results of Fig. 5.

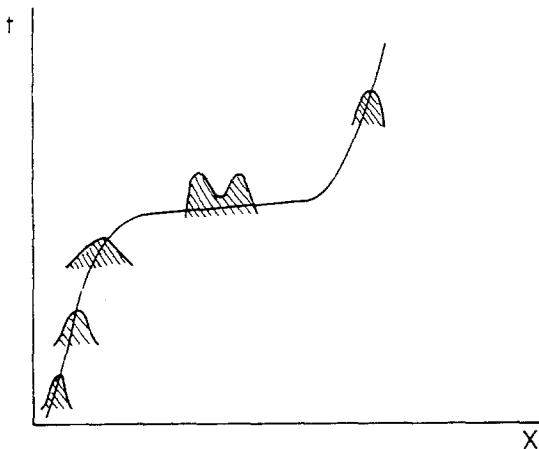


Fig. 8. A qualitative view of the phenomenon of transient bimodality.

4. THERMAL IGNITION IN A SPATIALLY DISTRIBUTED SYSTEM

Consider now a slab of length $2L$ in which a single first-order irreversible exothermic reaction is taking place. The deterministic mass and energy balance equations are

$$\frac{\partial \bar{c}}{\partial t} = -k_0 \bar{c} \exp\left(\frac{-U}{R\bar{T}}\right) + D_c \frac{\partial^2}{\partial r^2} \bar{c} \tag{21a}$$

$$\frac{\partial \bar{T}}{\partial t} = \frac{Q}{\rho C_V} k_0 \bar{c} \exp\left(\frac{-U}{R\bar{T}}\right) + D_T \frac{\partial^2}{\partial r^2} \bar{T} \tag{21b}$$

In addition to the notation introduced already in Eq. (1), D_c and D_T represent, respectively, the mass and thermal diffusivities of the reactant.

It will be convenient to switch to dimensionless variables,

$$\xi = r/L; \quad \bar{x} = \bar{c}/c_0; \quad \bar{\theta} = \bar{T}/T_0 \tag{22a}$$

where c_0 and T_0 are the initial concentration and temperature, respectively. We assume that

$$U/RT_0 = 1/\varepsilon' \gg 1; \quad D_T = D_c \tag{22b}$$

and introduce the characteristic diffusion and reaction times

$$t_D = L^2/D_T = L^2/D_c; \quad t_{ch} = k_0^{-1} \exp(1/\varepsilon') \tag{22c}$$

Moreover, we limit ourselves for simplicity to a closed system (adiabatic explosion). Equations (21a) and (21b) thus take the final form⁽¹⁷⁾

$$\frac{\partial}{\partial t} \bar{x} - \frac{1}{t_D} \frac{\partial^2}{\partial \xi^2} \bar{x} = -\bar{x} \frac{1}{t_{ch}} \exp\left(\frac{1}{\varepsilon'} - \frac{1}{\varepsilon' \bar{\theta}}\right) \tag{23a}$$

$$\frac{\partial}{\partial t} \bar{\theta} - \frac{1}{t_D} \frac{\partial^2}{\partial \xi^2} \bar{\theta} = (\theta_{ad} - 1) \bar{x} \frac{1}{t_{ch}} \exp\left(\frac{1}{\varepsilon'} - \frac{1}{\varepsilon' \bar{\theta}}\right) \tag{23b}$$

$$-1 \leq \xi \leq 1$$

supplemented with the zero-flux boundary conditions

$$\left(\frac{\partial \bar{x}}{\partial \xi}\right)_{\pm 1} = 0; \quad \left(\frac{\partial \bar{\theta}}{\partial \xi}\right)_{\pm 1} = 0 \tag{23c}$$

The ‘‘adiabatic temperature’’ θ_{ad} featured in Eq. (23b) is related to the maximum temperature that would be attained once the reaction is com-

pleted in a spatially uniform system. It is determined by energy conservation,

$$\rho C_V T_{\max} = \rho C_V T_0 + Q c_0 = \rho C_V T_0 \left(1 + \frac{Q}{\rho C_V} \frac{c_0}{T_0} \right)$$

or

$$\theta_{\text{ad}} = \frac{T_{\max}}{T_0} = 1 + \frac{Q}{\rho C_V} \frac{c_0}{T_0} \quad (24)$$

In what follows we fix the adiabatic explosion parameters to the values $T_0 = 800\text{K}$, $T_{\max} = 2000\text{K}$, $U/R = 10^4$, $\varepsilon' = 0.08$. This gives $\theta_{\text{ad}} = 2.5$ and an ignition temperature of $\theta_{\text{cr}} = 2$.

We now augment Eqs. (23a)–(23c) by adding fluctuations. As in Section 2, we describe their effect by adding to their right-hand sides random forces $F_x(\xi, t)$ and $F_\theta(\xi, t)$ representing Gaussian white noises in both space and time:

$$\begin{aligned} \langle F_x(\xi, t) \rangle &= 0; & \langle F_\theta(\xi, t) \rangle &= 0 \\ \langle F_x(\xi, t) F_x(\xi', t') \rangle &= \varepsilon Q_x \delta(\xi - \xi') \delta(t - t') \\ \langle F_\theta(\xi, t) F_\theta(\xi', t') \rangle &= \varepsilon Q_\theta \delta(\xi - \xi') \delta(t - t') \\ \langle F_x(\xi, t) F_\theta(\xi', t') \rangle &= 0 \end{aligned} \quad (25)$$

The variances Q_x and Q_θ must be fixed to satisfy a nonequilibrium fluctuation-dissipation theorem extending Eqs. (7) and (9) to spatially distributed systems. It should also be noted that if $F_x(\xi, t)$ and $F_\theta(\xi, t)$ are to represent thermodynamic fluctuations, they should contain two pieces: one scalar contribution appearing in Eqs. (25) in an additive fashion, and a second one associated with the divergence of the random part of the diffusive flux.^(15,16) In what follows, however, we treat Q_x and Q_θ as parameters and do not perform this decomposition explicitly. From this point on, therefore, F_x and F_θ should be looked at as stochastic perturbations of external origin.

Figure 9 describes the successive steps leading, in the absence of fluctuations, to a uniform temperature profile following an initial inhomogeneous perturbation at the center of the slab. We observe an initial stage of slow evolution followed by a fast increase of temperature throughout the slab, in agreement with Fig. 4. At $t = 0.07$ the entire system has reached a temperature at least equal to the ignition temperature $\theta_{\text{cr}} = 2$. In the representation of Fig. 4 this corresponds to the inflection point of the temperature versus time curve.

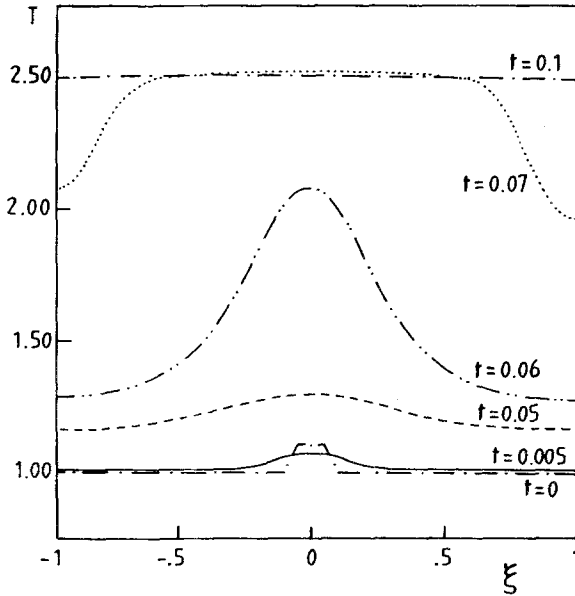


Fig. 9. Successive steps leading, in the absence of fluctuations, to a uniform temperature profile following an initial inhomogeneous perturbation at the center of the slab. Parameter value: $\epsilon' = 0.08$.

5. FLUCTUATION-INDUCED SYMMETRY BREAKING AND HOT SPOT STATISTICS

Figure 10 reports the behavior of a particular realization of the stochastic process obtained by adding fluctuations in Eqs. (23a)–(23c). Despite the small value of the variance chosen ($\epsilon Q_g = \epsilon Q_x = 0.001$), we observe strong deviations from the deterministic behavior. Specifically, while for t small the slab remains practically homogeneous, close to the critical (ignition) time strong inhomogeneities are spontaneously developed. Actually, there is a wide dispersion from one sample to another: while in the realization of Fig. 10 the temperature first reaches high values close to the middle part of the slab, in other realizations the maximum may be reached in the left or in the right boundary.

A first visualization of the overall spatial organization of the system is provided by Fig. 11. The system is divided into 20 cells and a great number of different realizations of the stochastic process is recorded. In each cell the number of times the temperature has exceeded the critical value $\theta_{cr} = 2$ is counted at any given instant, and the corresponding probability $P(\theta \geq \theta_{cr})$ is deduced as a function of both space and time. We observe that

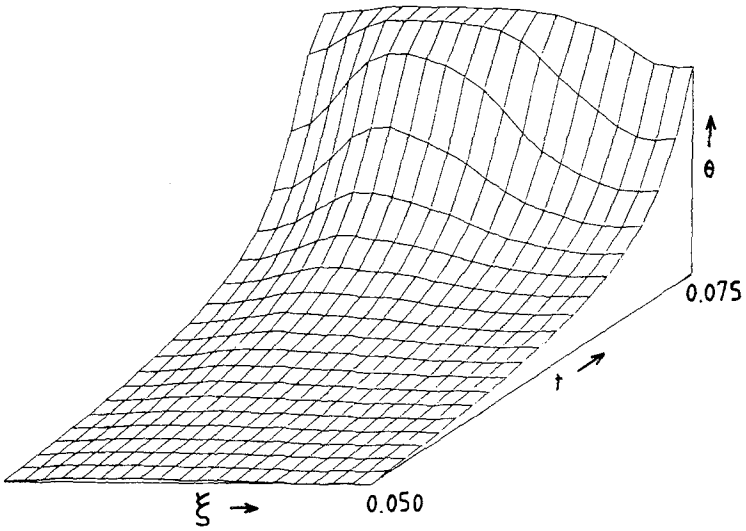


Fig. 10. A particular realization of the stochastic process obtained by adding fluctuations in Eqs. (23a)–(23c). Parameter values as in Fig. 9, with, in addition, $\varepsilon Q_x = \varepsilon Q_\theta = 0.001$.

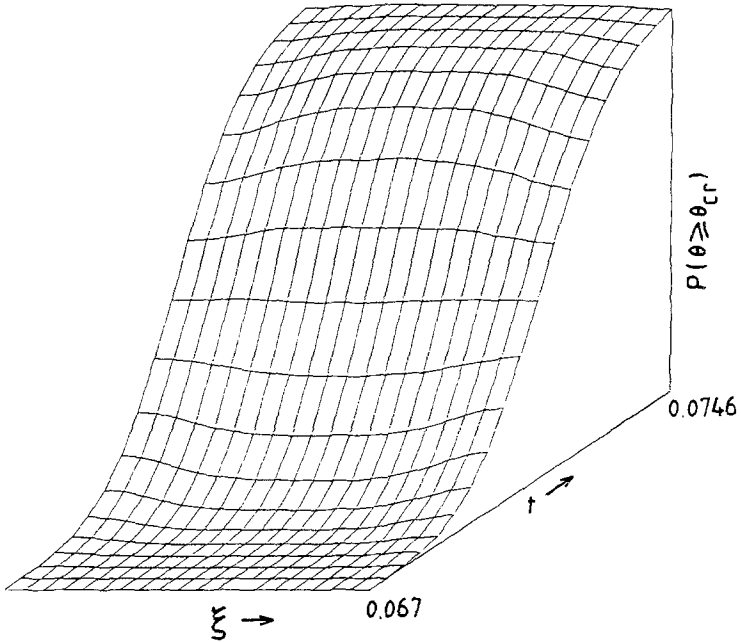


Fig. 11. Different stages of the spatial organization of a one-dimensional system undergoing thermal explosion in the presence of fluctuations. Notice the fluctuation-induced space symmetry-breaking during a time interval around explosion. Parameter values: $\varepsilon' = 0.08$, $\theta_{cr} = 2$.

prior to explosion the system remains homogeneous. However, during a time interval close to explosion (≈ 0.07 time units) the system develops systematic inhomogeneities at the macroscopic level. The inhomogeneities start because of the relatively higher probability to explode near the boundaries, since diffusion as a mechanism of heat removal is half as effective as elsewhere (zero-flux boundary conditions). Subsequently, however, the probability to have exploded becomes higher in the middle. Eventually, uniformization is taking place, and at 0.075 time units the entire slab is practically at the final temperature (compare to Fig. 9).

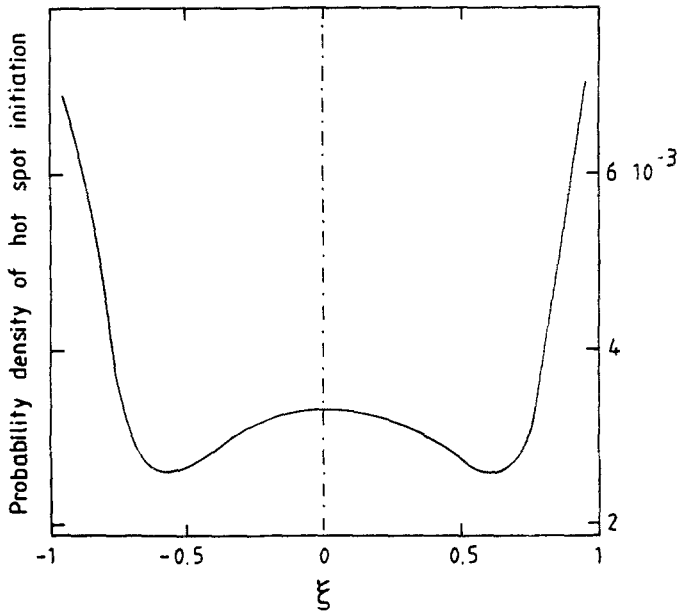
A particularly relevant piece of information—especially for the purpose of comparing with real-world experiments—is to record the probability that explosion has been *initiated* at a given point in space, whatever the value of the time of this particular explosion and the subsequent evolution of the system might have been. The complementary information of having the probability for the system to explode at a given time, whatever the space region in which explosion has first occurred might be, would also be desirable. Figure 12 depicts these two functions. In Fig. 12a we observe a rather striking spatial dispersion of the *hot spots* that initiate the explosion process. Figure 12b, to be compared with Fig. 5, shows that a dispersion of ignition times is likewise expected. However, it exhibits in its details some differences with the dispersion obtained in the preceding section: first, the ignition time probability is practically symmetric around the deterministic value of ignition time; and second, the dispersion is less pronounced than in the Semenov case. The main reason for this difference is that the value of $\varepsilon' = 0.08$ chosen in the numerical simulation is still relatively high, so that the adiabatic explosion does not exhibit an induction period as pronounced as the explosion near a limit point. Still, Eq. (20) provides a reasonable estimate: for $\varepsilon Q_\theta = 10^{-3}$ and $\alpha \approx 1$ (the values corresponding to the numerical simulations) one obtains a relative dispersion of about 0.02, in good qualitative agreement with the results reported in Fig. 12b.

The spatial differentiation revealed in Figs. 10, 11, and 12a can be further characterized by computing the time development of the space correlation function,

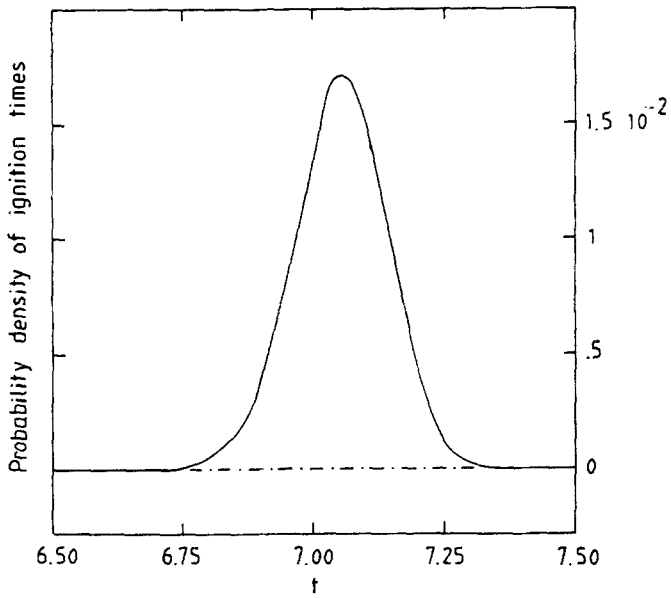
$$C_i(2, j) = \langle \delta T(2) \delta T(j) \rangle_i / \langle \delta T^2(2) \rangle_i; \quad j = 2, \dots, n \quad (26)$$

where j denotes a discretized space coordinate running through the system. To avoid spurious effects, the first lattice point after the left boundary is discarded.

The system is again started with a uniform initial condition. For time intervals around the explosion one then finds the behavior depicted in



(a)



(b)

Fig. 12. (a) Spatial dispersion of the first hot spot initiated in the system and (b) temporal dispersion of the first ignition event under the same conditions as in Fig. 11.

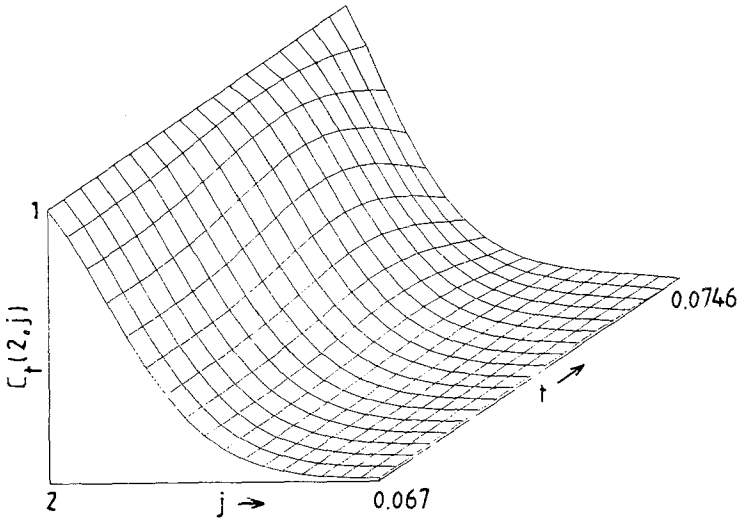


Fig. 13. Time evolution of the normalized temperature space correlation function under the same conditions as in Figs. 11 and 12.

Fig. 12. On the one side, the correlation function becomes nonuniform and decays monotonically with distance. But on the other side, it maintains a rather invariant profile throughout the explosion stage, showing only a slight enhancement in the immediate vicinity of the explosion time. This indicates a high degree of spatial coherence between macroscopically distant parts of the system, despite the complete absence of correlations of the noise source in space. In a sense, the initial deviation from equilibrium acts like a constraint inducing long-range order, in a way analogous to what is found in the study of correlations around nonequilibrium steady states.⁽¹⁸⁾

6. DISCUSSION

The theoretical explanation of the increased sensitivity of explosive systems to fluctuations remains fragmentary. The evaluation of the first and second moments of the passage time probability using a more realistic model than in Section 3 would be desirable. As for the behavior of spatially distributed systems, the effect of the system's size, of the boundary conditions, and of the geometry remains to be investigated. Moreover, the role of the dimension of the hot spot initiated by a fluctuation in its subsequent evolution should be assessed.

The phenomenon of transient bimodality has recently been verified experimentally in electrical⁽¹⁹⁾ and in optical⁽⁴⁾ systems. It would be impor-

tant to undertake a systematic experimental study of thermal combustion from a similar standpoint. Our analysis of spatially distributed systems is likely to be especially relevant in this context. It could provide a rational basis for understanding the pronounced variability of the phenomenon of combustion observed routinely in many experimental situations but attributed ordinarily to parasitic effects or to experimental imperfections.

ACKNOWLEDGMENTS

The research reported in this paper is supported in part by the European Communities under contract number STI-070-J-C (CD) and by the International Solvay Institutes of Physics and Chemistry.

REFERENCES

1. D. A. Frank-Kamenetskii, *Diffusion and Heat Transfer in Chemical Kinetics* (Plenum Press, New York, 1969).
2. A. Zettlemoyer (ed.), *Nucleation* (Dekker, New York, 1969).
3. G. Broggi and L. A. Lugiato, *Phil. Trans. R. Soc. Lond. A* **313**:425 (1984).
4. W. Lange, F. Mitschke, R. Deserno, and J. Mlynek, *Phys. Rev. A* **32**:1271 (1985).
5. R. May, *Stability and Complexity in Model Ecosystems* (Princeton University Press, Princeton New Jersey, 1973).
6. G. Nicolis and I. Prigogine, *Self-Organization in Non-equilibrium Systems* (Wiley, New York, 1977).
7. P. Bergé, Y. Pomeau, and C. Vidal, *Deterministic Chaos* (Herman, Paris, 1984).
8. N. V. Kondratiev and E. Nikitin, *Gas-Phase Reactions* (Springer-Verlag, Berlin, 1981).
9. G. Dewel, P. Borckmans, and D. Walgraef, *J. Phys. Chem.* **88**:5442 (1984).
10. T. Boddington, J. Griffiths, and K. Hasegawa, *Combustion Flame* **55**:297 (1984).
11. F. Baras, G. Nicolis, M. Malek Mansour, and J. W. Turner, *J. Stat. Phys.* **32**:1 (1983); G. Nicolis, F. Baras, and M. Malek Mansour, in *Non-equilibrium Dynamics of Chemical Systems*, C. Vidal and A. Pacault, eds. (Springer-Verlag, Berlin, 1984).
12. F. Baras, Ph. D. Dissertation, University of Brussels (1985).
13. N. G. Van Kampen, *Stochastic Processes in Physics and Chemistry* (North-Holland, Amsterdam, 1981).
14. M. Malek Mansour, C. Van den Broeck, G. Nicolis, and J. W. Turner, *Ann. Phys. (N.Y.)* **131**:283 (1981).
15. C. W. Gardiner, *Handbook of Stochastic Methods* (Springer-Verlag, Berlin, 1983).
16. L. D. Landau and E. M. Lifshitz, *Fluid Mechanics* (Pergamon Press, Oxford, 1959).
17. T. Boddington, C. G. Feng, and P. Gray, *Proc. R. Soc. Lond. A* **391**:269 (1984).
18. G. Nicolis and M. Malek Mansour, *Phys. Rev. A* **29**:2845 (1984).
19. E. Arimondo, D. Dangoisse, and L. Fronzoni, *Europhys. Lett.*, in press.